Final Technical Report for

PISCEES: Predicting Ice Sheet and Climate Evolution at Extreme Scales

June 15, 2012 – June 14, 2017

Florida State University	PI: Max Gunzburger	Grant number DE-SC0008273-ER65391
University of South Carolina	PI: Lili Ju	Grant number DE-SC0008087-ER65393

This report provides a summary of major accomplishments and activities obtained/performed by the Florida State University/University of South Carolina team participating in the PISCEES project. Further details about the results presented in this report can be found in the publications listed in Section 3.

The USC/FSU team members include Max Gunzburger (FSU, Institute Lead PI), Lili Ju (USC, Institute Lead PI), Tong Zhang (USC, Postdoc), Mauro Perego (FSU, Postdoc), Luca Bertagna (Postdoc), Wei Leng (USC and FSU, Visiting Scholar), Liyong Zhu (USC, Visiting Scholar) , Yan Xie (FSU, Visiting Scholar)

Contents

1. Accomplishments

In this section, major accomplishments for development and application of the prallell 3D finite element Stokes dycore "FELIX-S" of the PISCEES project are discussed in certain detail and some representative test results and findings are also provided.

1.1. A Picard-Newton finite element Stokes solver for ice-sheet dynamics

The Picard iteration is robust with respect to the initial guess for the solution, but is at best linearly convergent for solving the nonlinear finite element Stokes system. Thus, it is time consuming for long-time and large-spatial scale simulations in practical applications, such as decades to century scale, whole-ice sheet simulations of Greenland and Antarctica. Newton-based nonlinear iterative solvers are putatively quadratically convergent but are much less robust with respect to the initial solution guess. Our approach is to first run the Picard iteration for a few steps to provide a good initial guess for the Newton iteration, which then takes over until the solution converges. This

hybrid approach provides a powerful and efficient tool for solving the nonlinear Stokes system. We implemented and tested the performance of our new Stokes ice dynamics solver in the FELIX-S model on several diagnostic, 3D ice-sheet experiments. Figure 1 shows convergence results of the pure Picard and Picard-Newton methods for ISMIP-HOM benchmark experiments A and C. After starting with several Picard iterations, the Newton method converges quadratically in every case. The Picard-Newton method generally takes 8-15 iterations to reduce the relative residual by 10^{-10}, whereas the pure Picard method almost always took 20-25 iterations to reach a much larger relative residual of 10^{-4}.

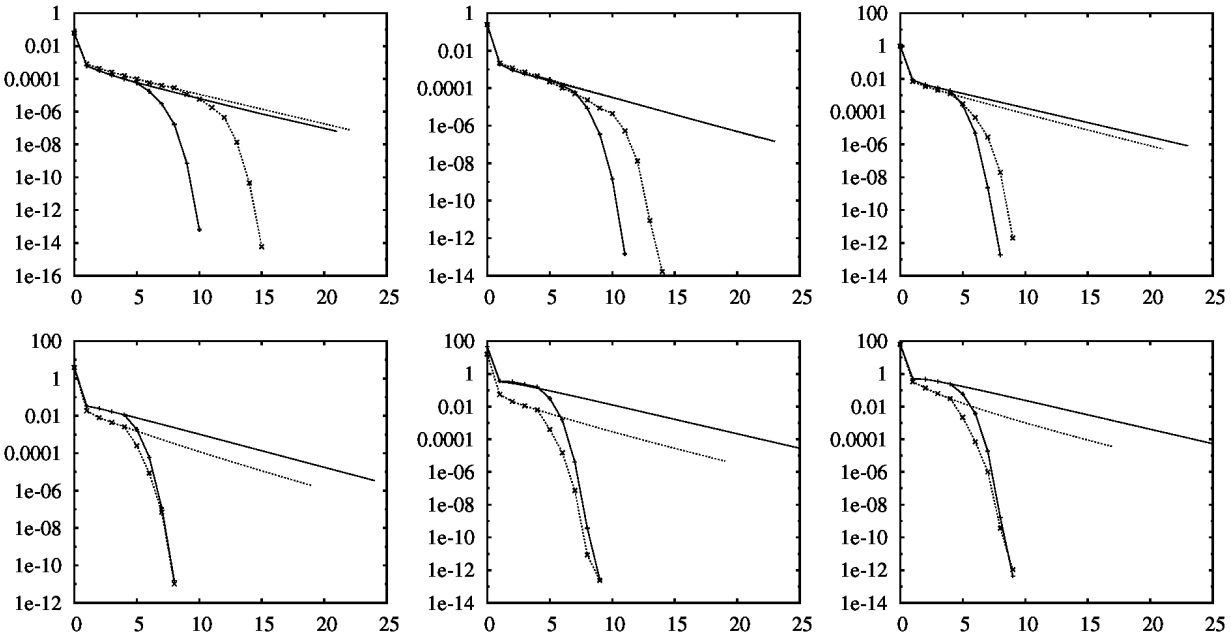

Figure 1: Convergence results of the pure Picard and Picard-Newton methods for ISMIP-HOM benchmark experiments A and C. From left to right and then from top to bottom: the ice-sheet horizontal length L= 5 km, 10 km, 20 km, 40 km, 80 km, 160 km. Solid lines: Exp. A with pure Picard method. Solid lines with asterisk: Exp. A with Picard-Newton method. Dashed lines: Exp. C with pure Picard method. Dashed lines with plus: Exp. C with Picard-Newton method.

1.2. A finite element ice-sheet temperature evolution solver and a finite volume ice-sheet thickness evolution solver

The temperature equation of ice sheet is advection-dominated in the horizontal directions and the melting point constraint needs to be satisfied throughout the 3D temperature field. We used cubic finite element temperature approximations and the SUPG-FEM (Streamline Upwind Petrov-Galerkin Finite Element Method) to stabilize the numerical scheme in our finite element ice-sheet temperature solver. The melting point constraint is treated using the nonlinear iterative method. The ice-sheet thickness evolution equation is a hyperbolic equation, and we implemented a upwinding finite volume solver that conserves the mass of the ice-sheet locally and globally. This property is often very important to simulation of long-time ice-sheet evolution. Combining the ice-sheet temperature and thickness solvers with the above Stokes solver for ice-sheet dynamics, we are able to simulate thermo-mechanically coupled ice-sheet evolution.

Figure 3 presents the results of the EISMINT-II benchmark experiments which are prognostic by our FELIX-S model. The overall model time step is limited by the advective CFL condition in the explicit Euler solution scheme for the ice-thickness evolution. We found a time step of 10 years

to be adequate for stability in the experiments discussed below. Exps. A, F, and G are run for 100,000 years and Exps. B, C, and D for 60,000 years; all experiments are run to an equilibrium state. On 256 processors, Exps. A, F, and G took about 48 hours to run and Exps. B, C, and D took about 24 hours (2000-2500 model years per wall-clock hour). For all experiments, the results by our computational model always show good stability and smoothness, remain radial symmetry during the whole evolution, and have quite significant differences with the results obtained by SIA models.

1.3. Development of a manufactured solution used for verification and validation

We developed a manufactured solution which is quite smooth and satisfies the compensated 3D Stokes equation and the boundary conditions; it is given as follows.

The geometry is that of an idealized rectangular slab of *isothermal* ice with length L and average thickness $Z = 1$km, resting on a sloping surface with a mean slope of $\alpha = 0.5^\circ$. Let $s_0(x, y) = -x\tan(\alpha)$. The fixed smooth basal topography is defined as a series of 500 m amplitude sinusoidal oscillations about the mean bed elevation:

$$b(x, y) = s_0(x, y) + \eta(x, y) - Z$$

with $\eta(x, y) = \frac{Z}{2}\sin\left(\frac{2\pi x}{L}\right)\sin\left(\frac{2\pi y}{L}\right)$. Due to ice-sheet flow and accumulation at the surface, the top surface of the ice sheet slowly evolves from flat with a uniform slope to a sinusoidal shape:

$$s(x, y, t) = s_0(x, y) + \eta(x, y)\xi(t)$$

with $\xi(t) = 1 - e^{-c_t t}$, where c_t is a parameter that controls the rate of ice thickness change. See Figure 3 for an sample illustration. The no-slip boundary condition is applied at the bottom basal surface, and periodic boundary conditions are applied on the lateral surfaces. Then, the manufactured solution is given by

$$\begin{aligned}
u(x, y, z, t) &= c_1\left[1 - \left(\frac{s - z}{s - b}\right)^4\right] \\
v(x, y, z, t) &= \frac{c_2}{s - b}\left[1 - \left(\frac{s - z}{s - b}\right)^4\right] \\
&\quad - \frac{1}{2}\frac{c_1}{s - b}\left[1 - \left(\frac{s - z}{s - b}\right)^4\right] Z\cos\left(\frac{2\pi x}{L}\right)\cos\left(\frac{2\pi y}{L}\right)e^{-c_t t} \\
w(x, y, z, t) &= u(x, y, z, t)\Big(\frac{\partial b}{\partial x}\frac{s - z}{s - b} + \frac{\partial s}{\partial x}\frac{z - b}{s - b}\Big) \\
&\quad + v(x, y, z, t)\Big(\frac{\partial b}{\partial y}\frac{s - z}{s - b} + \frac{\partial s}{\partial y}\frac{z - b}{s - b}\Big) \\
p(x, y, z, t) &= -2\eta_{\mathbf{u}}\frac{\partial u}{\partial x} - 2\eta_{\mathbf{u}}\frac{\partial v}{\partial y} + \rho g(s - z),
\end{aligned}$$

where c_1 and c_2 are parameters the user can choose to ensure that the velocity falls within a reasonable range. We used our manufactured solution to verify our FELIX-S model. Simulation results from the computational model show excellent, high-order accurate convergence of the computational model results to the manufactured exact solution. Manufactured solution technique is often used for the verification of computational models in many fields. The manufactured solution for the 3D Stokes ice-sheet model we developed can be used by all groups developing such models to verify their models. Furthermore, the manufactured solution provides an excellent setting for comparing

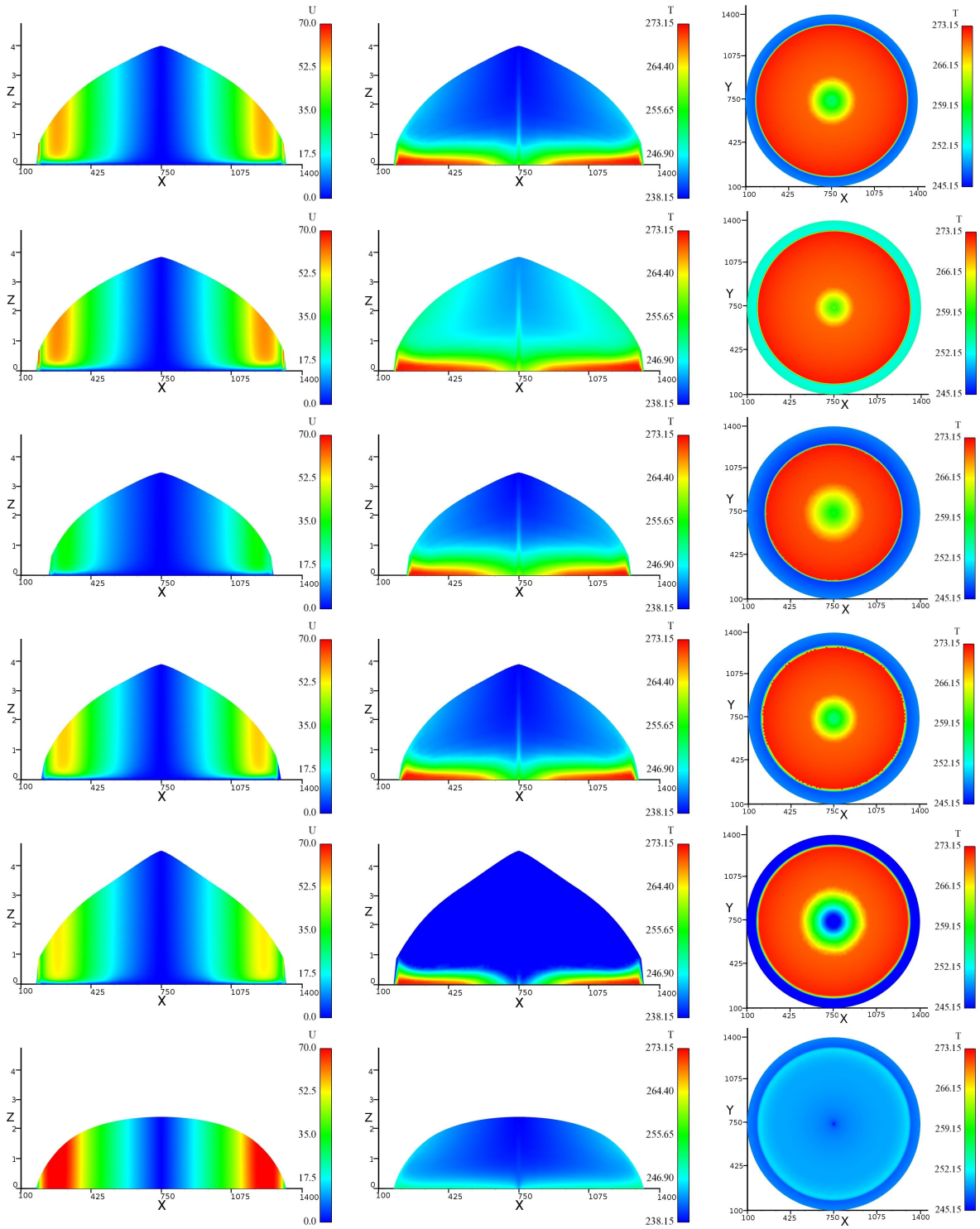

Figure 2: Steady state results for the EISMINT-II experiments by our FELIX-S model on an unstructured tetrahedral grid. From left to right: the velocity magnitude on the xz-plane, the temperature (K) on the xz-plane, and the basal temperature on the xy-plane. From top to bottom: Exps. A, B, C, D, F, and G.

the fidelity of different computational models so that it provides a valuable tool for assessing the relative usefulness of those models. Furthermore, because code verification is often a necessarily

step for the validation of mathematical models, the manufactured solution provides an avenue for model validation as well.

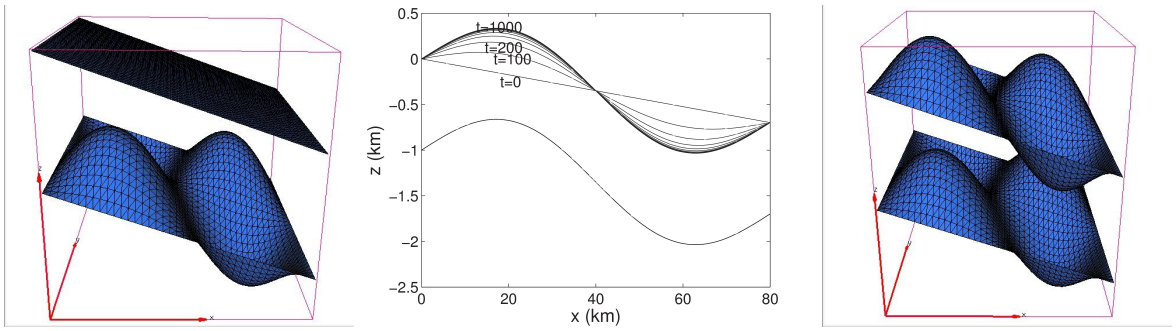

Figure 3: Illustration of the ice-sheet geometry (the top and bottom surfaces) of the manufactured Stoke solution at the time $t = 0$ (left) and at the time $t = 1000$ years (right). The middle figure is the x-direction profiles taken at $y = L/4$ of the ice-sheet top and bottom surfaces at 100 year time intervals from $t = 0$ to 1000 years.

1.4. Verification of 2D first-order flowline model

For many regions, glacier inaccessibility results in sparse geometric datasets (e.g., along the central flowline (CL) only) for use as model initial conditions. In these cases, two-dimensional flowline models are often used to study glacier dynamics. Therefore, we systematically investigated the applicability of a 2D, first-order Stokes approximation flowline model (FLM), modified by shape factors, for the simulation of land-terminating glaciers by comparing it to a 3D, "full" Stokes ice flow model (FSM) (represented by our FLEIX-S model). We explored the sensitivities of the FLM and FSM to ice geometry, temperature, and forward model integration time. We found that, compared to the FSM, the FLM generally produces slower horizontal velocities due to the simplifications inherent in the FLM and to the underestimation of the shape factor (see Figure 4). For polythermal glaciers, those with temperate ice zones, or when basal sliding is important, we found significant differences between simulation results when using the FLM versus the FSM (see Figure 5). Over time, initially small differences between the FLM and FSM become much larger near the cold-temperate ice transition surfaces. Long time integrations further increase small initial differences between the two models. We conclude that the FLM should be applied with caution when modeling glacier changes under a warming climate or over long periods of time.

1.5. Implementation of the ice shelf dynamics modeling

Compared to the grounded parts of an ice sheet, the ice shelf experiences different boundary conditions at its lower surface: (i) normal stress is equal to the buoyancy sea water pressure, and (ii) the tangential friction is assumed to be zero. The variational form of the Stokes model, including the ice shelf boundary conditions, now becomes

$$\begin{cases} \displaystyle\int_{\Omega_t} 2\eta_{\mathbf{u}_h}\dot{\boldsymbol{\varepsilon}}_{\mathbf{u}_h} : \dot{\boldsymbol{\varepsilon}}_{\mathbf{v}_h}\, d\mathbf{x} + \int_{\Gamma_{b,sld}} \beta^2 \mathbf{u}_h \cdot \mathbf{v}_h\, ds + \int_{\Gamma_w} P_w \mathbf{v}_h \cdot \mathbf{n} ds - \int_{\Omega_t} p_h \nabla \cdot \mathbf{v}_h\, d\mathbf{x} = \rho \int_{\Omega_t} \mathbf{g} \cdot \mathbf{v}_h\, d\mathbf{x}, \\ \displaystyle -\int_{\Omega_t} q_h \nabla \cdot \mathbf{u}_h\, d\mathbf{x} = 0. \end{cases}$$

where Γ_w denotes the part of ice shelf surface having contact with sea water and P_w the water pressure. Note that, to remove the numerical instability arising from the small hydrostatic disequilibrium, we need to take account of the surface change in the integration time step when computing the normal stress at the ice shelf bottom:

$$\sigma_{\mathrm{nn}}(t) = \rho_{\mathrm{w}} g z_{\mathrm{b}}(x, y, t),$$

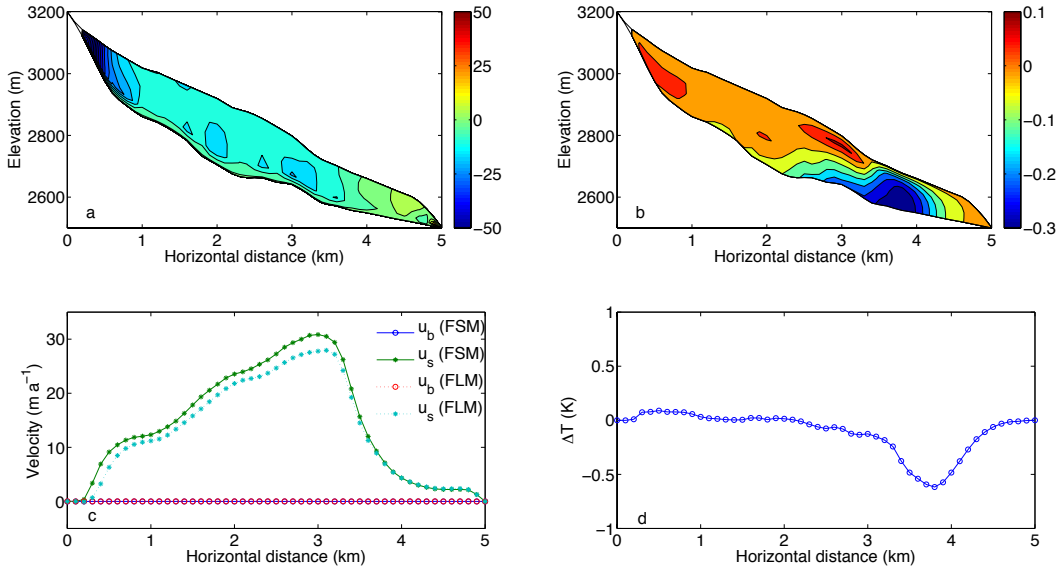

Figure 4: Steady state thermomechanically decoupled model results for the Haut Glacier d' Arolla geometry with parabolic cross-sections. (a) relative horizontal velocity error (r_u) distribution; (b) relative temperature error (r_T) distribution; (c) surface (u_s) and basal velocity (u_b) of the FSM and the FLM along the CL; (d) difference of the mean column ice temperature between FSM and FLM ($\Delta T = \bar{T}_{\mathrm{FLM}} - \bar{T}_{\mathrm{FSM}}$) along the CL.

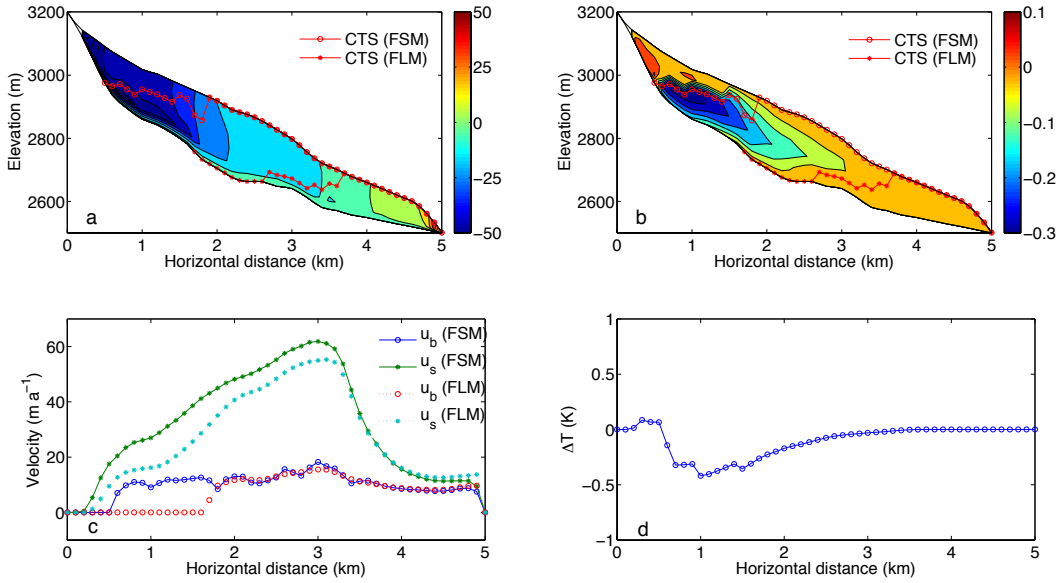

Figure 5: Steady state thermomechanically coupled model results for the Haut Glacier d' Arolla geometry with parabolic cross-sections. (a) relative horizontal velocity error (r_u) distribution (absolute values larger than 50 % are not shown); (b) relative temperature error (r_T) distribution; (c) surface (u_s) and basal velocity (u_b) of FSM and FLM along the CL; (d) difference of the mean column ice temperature between FSM and FLM ($\Delta T = \bar{T}_{\mathrm{FLM}} - \bar{T}_{\mathrm{FSM}}$) along the CL. CTS represents the cold-temperate ice transition surface.

where ρ_{w} is the sea water density, g is the acceleration of gravity and z_{b} is the elevation at the ice shelf bottom (the sea level is set to 0 m), which can be described as

$$z_{\mathrm{b}}\left(x,y,t\right)=z_{\mathrm{b}}\left(x,y,t-\mathrm{d}t\right)+\mathbf{u}\cdot\mathbf{n}\sqrt{1+\left(\partial z_{\mathrm{b}}/\partial x\right)^{2}+\left(\partial z_{\mathrm{b}}/\partial y\right)^{2}}\mathrm{d}t.$$

We should also note that large geometry changes may commonly appear around the grounding line where two different boundary conditions intersect. In order to further stabilize the numerical schemes used in the FELIX-S model, it is highly necessary to average/smooth the outer normal values of the bottom faces near the grounding line. In addition, a consistent pattern of coordinate rotation scheme is also strongly required for both the lower grounded and floating surfaces when different boundary conditions are applied. To verify our model ability for simulating ice shelf dynamics, we ran a diagnostic inter-comparison test with Elmer/Ice and found they are generally consistent (see Figure 6).

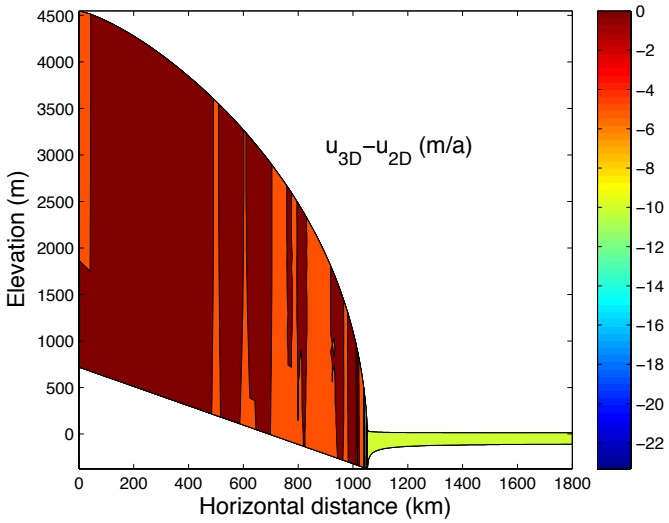

Figure 6: Comparison of horizontal velocity between Elmer/Ice (2D) and our model (3D).

1.6. Contact problem for grounding line migration

For the grounded element faces that lie below the sea level, there are two competing forces: sea water pressure that is lifting the ice up and the gravity that drives ice flow down. To get the idea of how many originally grounded faces at the bottom will now become afloat, we first need to evaluate the magnitude of water pressure and internal stress exerted on them, which has been implemented in two different ways in our FELIX-S model:

1. Following Elmer/Ice, we compute the "nodal force", F_{w}, exerted on the bottom faces by the ocean by integrating the sea pressure over the element faces, as is inherent in the finite element method. The so called "contact force", R, exerted by the internal stress, is obtained by computing the residual of Stokes system by removing the Dirichlet boundary condition at the grounded bottom faces. The magnitude of nodal and contact forces, both face averaged variables, are then compared: (i) if $|F_{\mathrm{w}}| >= |R|$, set the element face mask to be floating; (ii) if $|F_{\mathrm{w}}| < |R|$, set the element face mask to be grounded. This method is quite handy. However, we here also offer another way:

2. We compute the normal stress (σ_{nn}) and water pressure (P_{w}) at the lower grounded faces and compare them directly. The normal stress is computed directly from the velocity field based

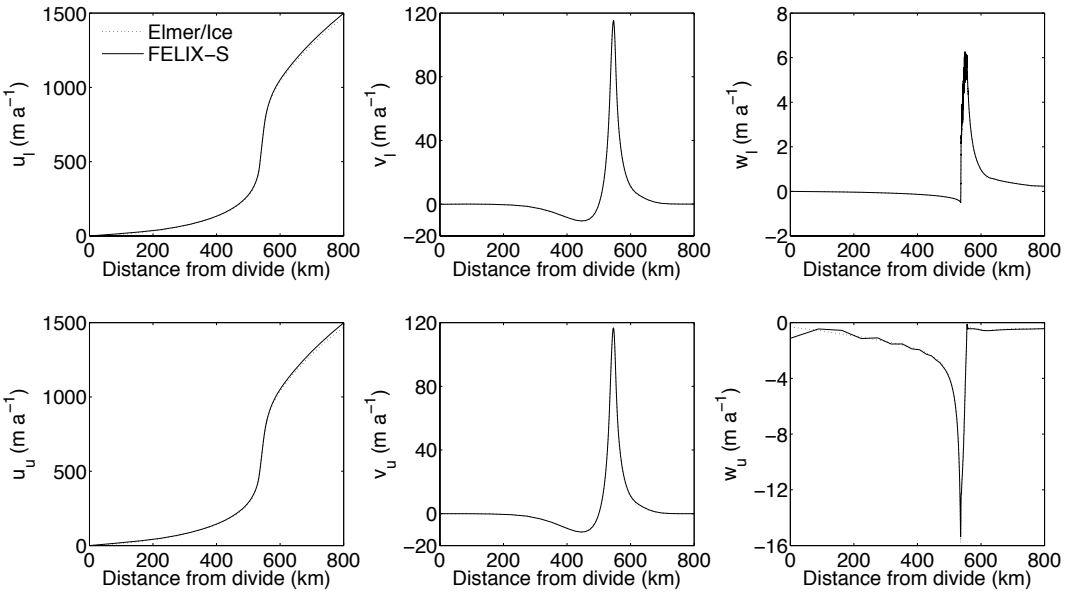

Figure 7: Comparisons of mean (along the y direction) velocities for upper (u_u, v_u and w_u) and lower surfaces (u_l, v_l, and w_l) along the x direction for FELIX-S (black solid line), Elmer/Ice FF (red dotted line), DI (black dotted line) and LG (blue dotted line) cases for the diagnostic experiment P75D. Where black dotted line is not clearly visible, Elmer/Ice and FELIX-S solutions are overlying.

on Glen's flow law. We here define a element face as floating only when $P_{\rm w} >= |\sigma_{\rm nn}|$ for all three nodes of it.

1.7. A comparison with Elmer/Ice for MISMIP3D

The Marine Ice Sheet Model Intercomparison for plan view models (MISMIP3d) contains benchmark experiments for Stokes and lower-order ice flow models. Based on our work during last year we conduct a detailed comparison with Elmer/Ice, another "full" Stokes model, on MISMIP3d for both diagnostic (P75D) and prognostic (Stnd, P75S and P75R) simulations.

We first compared the two models for the diagnostic experiment, P75D (Figure 7). Both models use the same parameters and, despite the different element types discussed above, have identical nodal coordinates over the entire model domain. From Figure 7, it is clear that the three velocity components (u, v and w) for Elmer/Ice and FELIX-S are in very good agreement for both the upper and lower surfaces, an indication of inherent consistencies between the two models (recall that the most direct comparison between Elmer/Ice and FELIX-S is using the DI results from Elmer/Ice). In general, for the horizontal velocity, u, the differences are relatively small near the ice divide and increase continuously from the grounding line (GL) to the ice shelf portion of the domain (Figure 8). For the v and w velocity components, we observe relatively larger discrepancies in the region of the GL (around km 535 – 555), but still very small differences ($< 5\%$) over the majority of the domain (Figure 8). Overall, we found that for the P75D experiment FELIX-S results in slightly larger horizontal velocities (u) at the GL than does Elmer/Ice. As a result, FELIX-S exhibits a slightly (1%) larger ice flux through the GL than does Elmer/Ice.

For the Stnd Prognostic experiment, FELIX-S uses the same initial ice sheet geometry and the same along-flow resolution (50 m) and mesh coordinates as Elmer/Ice. Both models demonstrate a continuous advance of the GL, with FELIX-S reaching a steady state GL position of 519.85 km and Elmer/Ice reaching steady state positions of GL position 529.55, 526.80 and 522.35 km (for LG, DI

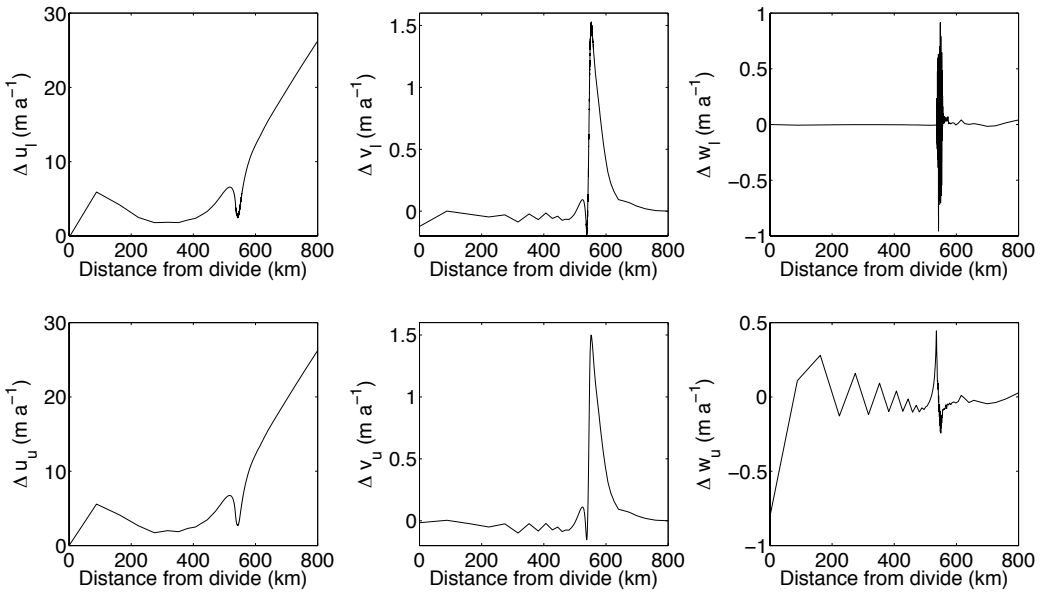

Figure 8: Comparisons of mean (along the y direction) velocity differences for upper (Δu_u, Δv_u and Δw_u) and lower (Δu_l, Δv_l and Δw_l) surfaces along the x direction for FELIX-S and Elmer/Ice for the diagnostic experiment P75D. The dotted, solid and dashed lines denote the differences by substrating Elmer/Ice LG, DI and FF values from FELIX-S values, respectively.

and FF, respectively). Apparently, FELIX-S produces a slightly smaller equlibrium-sized ice sheet with a GL position that is slightly more retreated than that of Elmer/Ice. This is consistent with the results from the diagnostic experiment, which show that overall, FELIX-S results in slightly higher along-flow velocities upstream from, at, and downstream from the GL (with the result of a slightly higher ice flux across the GL, slightly thinner ice there, and hence floatation occurring slightly farther inland). We have also experimented with finding the steady-state geometry and GL position for FELIX-S by letting the ice sheet retreat from an initially over-sized configuration, with a GL far advanced from its equilibrium position (rather than starting from an under-sized configuration and advancing to its equilibrium position). In this case, we found a GL position of 524.50 km, a circa 5 km difference with the advancing case, which is consistent with the 2D MISMIP-3a experiments conducted by Elmer/Ice. As they found, we expect that the steady-state GL locations from an advanced or retreated initial condition converge as the grid resolution increases.

In the P75S and P75R prognostic experiments, we investigated advance and retreat of the GL following a step-change perturbation in the basal friction distribution, for 100 years, and a return to the initial basal friction distribution, for a further 100 years (the "S" and "R" experiments, respectively). We start from the steady-state GL position of the Stnd prognostic experiment. Note that, because of the different GL positions and refined meshes in the vicinity of GL. Similar to the Stnd prognostic experiment, FELIX-S predicts relatively less GL advance (P75S) and more GL retreat (P75R) than Elmer/Ice, as shown in Figures 9-11. Similar to Elmer/Ice, FELIX-S shows a clear sensitivity to *across-flow* resolution (Δy); as the number of elements in the y direction increases from 20 to 80, the "reversibility" – i.e. the return to the initial position – of the GL improves (Figures 9-11). Importantly, we also found that as the number of elements in the y direction increases from 20 to 80, the agreement between FELIX-S and Elmer/Ice increases for *all*

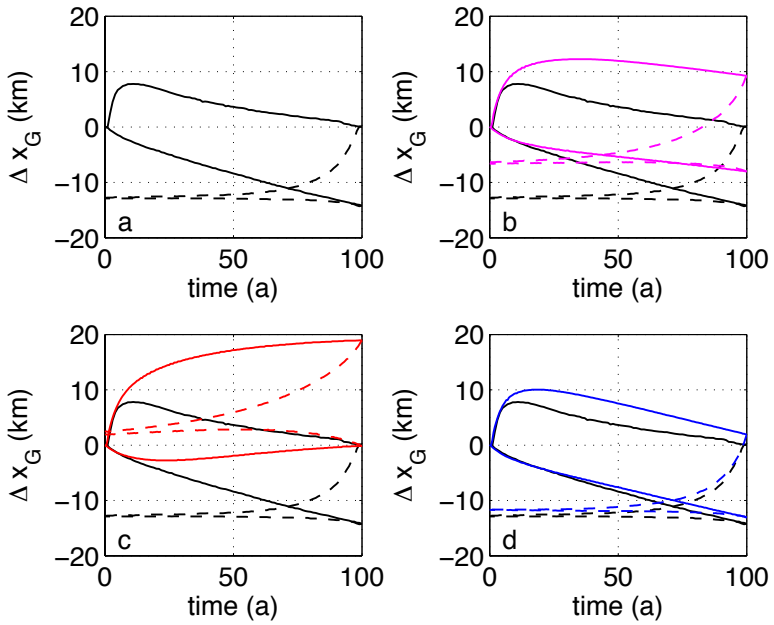

Figure 9: GL evolutions on both the symmetry axis (top curves) and free-slip boundary (bottom curves) for the P75S (solid curves) and P75R (dashed curves) comparisons among FELIX-S (a; black curves), Elmer/Ice DI (b; magenta curves), LG (c; red curves) and FF (d; blue curves). The element number along y is 20.

GL implementations used by Elmer/Ice (i.e., LG, DI, and FF). Based on the related observation in Elmer/Ice that the steady-state GL positions for LG, DI, and FF converge as grid resolution increases, we conclude that FELIX-S and Elmer/Ice show convergence of steady-state groundling line positions for the P75S and P75R experiments with increasing grid resolution.

1.8. Well posedness of a coupled ice-hydrology problem arising in glaciology

As a start towards the development of a coupled ice-hydrology problem, we have studied mathematical properties of a coupled dycore/hydrology model. The description of the movement of ice sheets such as Antarctica and Greenland features mathematical challenges such as the nonlinear dependence of the ice viscosity on the ice velocity and the complex interaction between the ice and the underlying bedrock. The latter is particularly difficult to model, given the difficulty of measuring quantities of interest at such deep locations. Perhaps the most widely accepted choice for modeling such interactions is a regularized Coulomb friction law introduced by Schoof that involves an additional unknown, namely the effective pressure at the ice-bedrock interface. This quantity can be modeled as the solution of an additional partial differential equation holding along the ice-bedrock interface that models the subglacial hydrology. In particular, for the ice we consider the Blatter-Pattyn (or first-order) model whereas for the subglacial hydrology model we use a quasi-static model first introduced by Hewitt. We proved the existence and uniqueness of the solution to the coupled ice-hydrology problem.

1.9. Efforts to merge FELIX-S into the existing ice flow model framework

Based on the achievements we have as described in the section above, we have tried to add the existed FELIX-S code into the CISM framework. On June, 2015, our group member Tong Zhang visited Sandia National Laboratories at Albuquerque, NM, for a tutorial of our Stokes ice sheet model code, FELIX-S, with other folks (Stephen Price and Matthew Hoffman) from Los Alamos

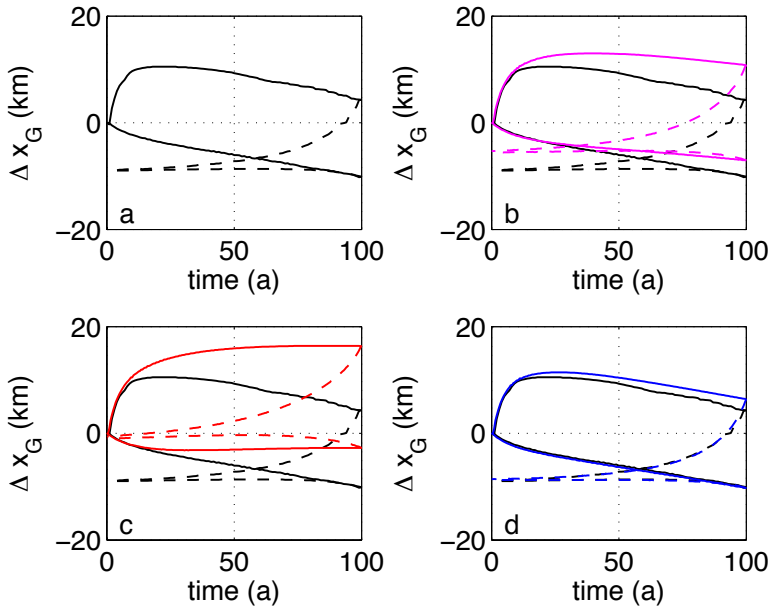

Figure 10: GL evolutions on both the symmetry axis (top curves) and free-slip boundary (bottom curves) for the P75S (solid curves) and P75R (dashed curves) comparisons among FELIX-S (a; black curves), Elmer/Ice DI (b; magenta curves), LG (c; red curves) and FF (d; blue curves). The element number along y is 40.

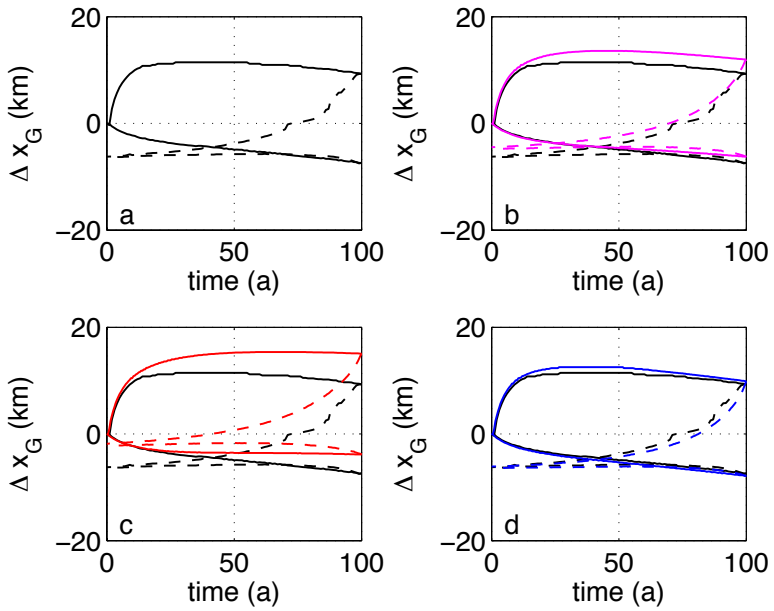

Figure 11: GL evolutions on both the symmetry axis (top curves) and free-slip boundary (bottom curves) for the P75S (solid curves) and P75R (dashed curves) comparisons among FELIX-S (a; black curves), Elmer/Ice DI (b; magenta curves), LG (c; red curves) and FF (d; blue curves). The element number along y is 80.

National Laboratory. During the two-day's stay, a through review of the usage of FELIX-S was taken, including the mesh generating method, model parameter setting, numerical experiment implementation, model runs and result visualization. The code is now saved as a repository on the node of NERSC server. Thus, one can use FELIX-S as a stand-alone code for ice sheet simulation. An interface between FELIX-S and other ice flow codes, for example, Albany/FELIX, is still underway.

2. Presentations

- *"Mathematical and numerical modeling of ice-sheet dynamics"*, Oak Ridge National Lab, June 2012 (by M. Perego)
- *"A parallel high-order accurate finite element nonlinear Stokes ice sheet model and benchmark experiments"*, Applied Mathematics Seminar, Department of Mathematics, Michigan State University, September 2012 (by L. Ju)
- *"The science of ice sheets: The mathematical modeling and computational simulation of ice flows"*, University of Oxford, United Kingdom, November 2012 (by M. Gunzburger)
- *"The science of ice sheets: The mathematical modeling and computational simulation of ice flows"*, Rostchild Lecture, Newton Institute for Mathematical Sciences, Cambridge University, United Kingdom, November 2012 (by M. Gunzburger)
- *"The science of ice sheets: The mathematical modeling and computational simulation of ice flows"*, SIAM Student Lecture, University of Florida, Gainesville, FL, February 2013 (by M. Gunzburger)
- *"Felix: advances in modeling forward and inverse ice-sheet problems"*, LIWG meeting at NCAR, Boulder, CO, February 2013 (by M. Perego)
- *"A finite element implementation of higher-order ice-sheet models: Mathematical and numerical challenges"*, SIAM CSE Conference, Boston, MA, February 2013 (by M. Perego)
- *"A parallel computational model for three-dimensional thermo-mechanical Stokes ow simulations of glaciers and ice sheets"*, SIAM Southeastern Atlantic Section Annual Meeting 2013, Knoxville-ORNL, TN, March 2013 (by L. Ju)
- *"A parallel computational model for three-dimensional thermo-mechanical Stokes flow simulations of glaciers and ice sheets"*, Seminar, School of Mathematical Sciences, University of Science and Technology of China, China, May 2013 (by L. Ju)
- *"A parallel computational model for three-dimensional thermo-mechanical Stokes ow simulations of glaciers and ice sheets"*, International Conference on Mathematical Modeling and Computation, Wuhan, China, May 2013 (by L. Ju)
- *"A parallel computational model for three-dimensional thermo-mechanical Stokes flow simulations of glaciers and ice sheets"*, Seminar, Laboratory of Computational Geodynamics, Graduate University of Chinese Academy of Sciences, June 2013 (by L. Ju)
- *"A parallel computational model for three-dimensional thermo-mechanical Stokes flow simulations of glaciers and ice sheets"*, Colloquium, Department of Mathematics and Statistics, Missouri University of Science and Technology, November 2013 (by L. Ju)
- *"A parallel computational model for three-dimensional thermo-mechanical Stokes flow simulations of glaciers and ice sheets"* , SIAM Southeastern Atlantic Section Annual Meeting 2014, Melbourne, FL, March 2014 (by L. Ju)

- *"The science of ice sheets: Modeling and computation of ice flows"*, Colloquium, Department of Applied Mathematics, University of Washington April 2014 (by M. Gunzburger)
- *"Suitability of the application of two dimensional thermo-mechanical ice flow model on mountain glaciers"*, 2014 CESM LIWG Workshop, The Village at Breckenridge, Breckenridge, CO, June 2014 (by T. Zhang)
- *"A parallel computational model for three-dimensional thermo-mechanical Stokes flow simulations of glaciers and ice sheets"*, Colloquium, Department of Mathematical Sciences, Shandong Normal University, China, June 2014 (by L. Ju)
- *"A parallel computational model for three-dimensional thermo-mechanical Stokes flow simulations of glaciers and ice sheets"*, International Workshop on the Frontiers of Computational Geodynamics, Beijing, China, July 2014 (by L. Ju)
- *"A parallel computational model for 3D thermo-mechanical Stokes flow simulations of ice sheets"*, Colloquium, Department of Mathematics, University of Alabama, September 2014 (by L. Ju)
- *"A parallel computational model for 3D thermo-mechanical Stokes flow simulations of ice sheets"*, Colloquium, Department of Mathematics and Statistics, Old Dominion University, October 2014 (by L. Ju)
- *"A parallel computational model for 3D thermo-mechanical Stokes flow simulations of ice sheets"*, Seminar, Chinese Network Information Center, Chinese Academy of Sciences, December 2014 (by L. Ju)
- *"The science of ice sheets: Modeling and computation of ice flows"*, Colloquium, Department of Mathematics, University of Houston February 2015 (by M. Gunzburger)
- *"A finite element three-dimensional stokes ice sheet dynamics model with enhanced local mass conservation"*, SIAM Conference on Computational Science and Engineering 2015, Salt Lake city, Utah, March 2015 (by L. Ju)
- *"MISMIP3d simulations using FELIX-S"*, 2015 CESM LIWG Workshop, The Village at Breckenridge, Breckenridge, CO, June 2015 (by T. Zhang)
- *"A finite element three-dimensional Stokes ice sheet dynamics model with enhanced local mass conservation"*, Workshop on Computational Mathematics and Scientific Computing, Jeju Island, Korea, August 2015 (by L. Ju)
- *"A parallel computational model for 3D thermo-mechanical stokes flow simulations of ice sheets"* , Applied Mathematics Seminar, George Washington University, Washington, DC, March 2015 (by L. Ju)
- *"Estimation of the coefficients in a coulomb friction boundary condition for ice sheet sliding on bedrocks"*, SIAM Conference on Uncertainty Quantification, Lausanne, Switzerland, April 2016 (by L. Bertagna)
- *"A parallel computational model for 3D thermo-mechanical Stokes flow simulations of ice sheets"*, Seminar, State Key Laboratory of Cryospheric Sciences, Chinese Academy of Sciences, May 2016 (by L. Ju)
- *"A parallel computational model for 3D thermo-mechanical Stokes flow simulations of ice sheets"*, Seminar, Department of Mathematical Sciences, Tsinghua University, China, June 2016 (by L. Ju)

- *"A parallel computational model for 3D thermo-mechanical Stokes flow simulations of ice sheets"*, Workshop on Current Tends in Numerical PDEs and Applications, Xi'an, China, December 2016 (by L. Ju)
- *"A parallel computational model for 3D thermo-mechanical Stokes flow simulations of ice sheets"*, CAM Seminar, Department of Mathematics, University of Tennessee at Knoxville, February 2017 (by L. Ju)

3. Publications

- W. Leng, L. Ju, M. Gunzburger, and S. Price, Manufactured solutions and the verification of three-dimensional Stokes ice-sheet models, *The Cryosphere*, Vol. **7**, pp. 19-29, 2013.
- W. Leng, L. Ju, M. Gunzburger and S. Price, A parallel computational model for three-dimensional, thermo-mechanical Stokes flow simulations of glaciers and ice sheets, *Communications in Computational Physics*, Vol. **16**, pp. 1056-1080, 2014.
- W. Leng, L. Ju, Y. Xie, T. Cui, and M. Gunzburger, Finite element three-dimensional Stokes ice sheet dynamics model with enhanced local mass conservation, *Journal of Computational Physics*, Vol. **274**, pp. 299-311, 2014.
- L. Ju, J. Zhang, L. Zhu and Q. Du, Fast explicit integration factor methods for semilinear parabolic equations, *Journal of Scientific Computing*, Vol. **62**, pp. 431-455, 2015.
- T. Zhang, L. Ju, W. Leng, S. Price and M. Gunzburger, Thermomechanically coupled glacier modeling for land-terminating glaciers: A comparison of two-dimensional, first-order and three-dimensional, full Stokes approaches, *Journal of Glaciology*, Vol. **61**, pp. 702-712, 2015.
- L. Zhu, L. Ju and W.-D. Zhao, Fast high-order compact exponential time differencing Runge-Kutta methods for second-order semilinear parabolic equations, *Journal of Scientific Computing*, Vol. **67**, pp. 1043-1065, 2016.
- T. Zhang, S. Price, L. Ju, W. Leng, J. Brondex, G. Durand and O. Gagliardini, A comparison of two Stokes ice sheet models applied to the Marine Ice Sheet Model Intercomparison Project for plan view models (MISMIP3d), *The Cryosphere*, Vol. **11**, pp. 179-190, 2017.
- L. Ju and Z. Wang, Exponential time differencing gauge method for incompressible viscous flows, *Communications in Computational Physics*, Vol. **22**, pp. 517-541, 2017.
- X. Yang and L. Ju, Efficient linear schemes with unconditionally energy stability for the phase field elastic bending energy model, *Computer Methods in Applied Mechanics and Engineering*, Vol. **315**, pp. 691-712, 2017.
- L. Bertagna and M. Gunzburger, Well posedness of a coupled ICE-Hyrdrology problem arising in glaciology, *SIAM Journal on Mathematical Analysis*, Vol. **49**, pp. 699-722, 2017.